Structure, Growth, and Morphology in Para Nitroaniline Dispersed Polymethyl Methacrylate Guest-Host NLO Composites

C. SAUJANYA, ANITA DHUMAL, ANJANA MITRA, S. RADHAKRISHNAN

Polymer Science and Engineering, National Chemical Laboratory, Pune 411008, India

Received 14 July 1998; accepted 31 December 1998

ABSTRACT: The structure, growth, and morphology of composite films made by dispersing para nitroaniline (PNA) in poly(methyl methacrylate) (PMMA) was investigated with respect to different crystallization methods, composition, and application of electric field. The wide-angle X-ray diffraction scans showed large variations in intensity of different reflections, especially the Okl with composition and in the presence of an electric field. In addition, it also showed the occurrence of a new crystalline structure, possibly due to complex formation between PNA and PMMA. The presence of this complex was further confirmed by infrared spectroscopy and thermal analysis. In a certain range of composition (30 to 40 % PNA), spherulitic morphology was observed, which otherwise consisted of needle-shaped crystals dispersed in amorphous matrix. The transparency of these films also depended strongly on the crystallization conditions, and highly transparent films could be obtained, even at high PNA content by application of electric field. These various results could be explained on the basis of the intermolecular interaction between PNA and PMMA, as well as preferential growth direction and orientation of the PNA crystals. © 1999 John Wiley & Sons, Inc. J Appl Polym Sci 74: 3522–3534, 1999

INTRODUCTION

Organic materials with controlled crystalline structure and morphology have drawn considerable attention in recent years because of their special properties, such as high conductivity, nonlinear optical properties, and liquid crystalline nature, which find application in electronics and optoelectronics.[1–4] However, for large area devices and ease in the processing of these, there have been attempts to incorporate them in polymeric matrices, such as polymethyl methacrylate (PMMA), polyvinyl alcohol (PVA), and polyethylene oxide (PEO).[5–7] The nonlinear optical (NLO) properties of paranitroaniline (PNA) dispersed in polymer as guest-host material has been extensively studied in the past.[8–11] However, these were restricted to very low concentration of PNA and mostly in the amorphous phase. In the previous studies, the authors have looked mainly at the electrical and optical properties[12–14] of para nitroaniline (PNA) dispersed polymers, and very little attention has been paid to the structural and morphological aspects. It is well known that crystalline structure, phase, and orientation play an important role in governing the nonlinear optical properties.[4,7] Further, modification of structure and morphology using polymeric media is also becoming increasingly important area for developing smart materials.[15,16] We have recently reported such polymer-induced crystallization effects in various materials, such as copper chloride and cadmium sulphide.[17–19] It was felt that similar effects could be used for developing orienta-

Correspondence to: S. Radhakrishnan.

Journal of Applied Polymer Science, Vol. 74, 3522–3534 (1999)
 CCC 0021-8995/99/143522-13

tion and ordered structure in such composites showing nonlinear optical (NLO) activity. Hence, we have investigated the structure, growth, and morphology of PNA dispersed in polymethyl methacrylate (PMMA), which is a widely used polymer in optical components. We report here the interesting morphological features observed in these composites under certain growth conditions.

EXPERIMENTAL

The PNA–PMMA films were firstly grown by a solution-casting technique and subsequently crystallized under different conditions. The required amount of PMMA (Gujpol, GSFC, Baroda) was dissolved in acetone (3 wt %), to which were added PNA (BDH England) solution in acetone in order to obtain different concentrations of the additive ranging from 10 to 45%. A small quantity of this solution (15 mL) was evaporated in flat glass petri dishes over 20 h at room temperature (28°C), giving solution-crystallized films. These films were pealed off the substrates, cut to size, and subjected to melt crystallization by placing them between the glass slides on a hot plate at a temperature of 200°C and transferred on to a hot stage at 60°C and held for a desired time, then followed by cooling to room temperature (melt-crystallized samples). Some of these films were crystallized under the influence of electric field, for which the 30 and 40% PNA–PMMA films were first coated on transparent conducting glass (ITO), which were then sandwiched to form a ITO–film–ITO type configuration. These were placed on hot plate held at 150°C and an electric field (12 V across 30 μm) was applied for 1 h. These were slowly cooled for another hour. The films were pealed off after soaking in water and dried as before. The structure, growth, and morphology of the PNA–PMMA films was investigated by wide-angle X-ray diffraction (WAX) and optical polarizing microscopy in the manner reported elsewhere.[20–22] A few films were also characterized by infrared (IR) spectroscopy and differential scanning calorimetry (DSC).

RESULTS AND DISCUSSION

The PNA-dispersed composite films grown from the solution-casting technique were flexible and transparent up to a PNA concentration of 30%, while those having a high concentration of PNA were brittle and opaque. This suggests that the film having low concentration of PNA could be amorphous or have a crystallite size much less than 1000 Å. This was confirmed by us by use of a optical polarizing microscopy. The transparency and quality of films depended very much on the technique and conditions used for growing them. These aspects will be discussed later in the article.

The crystalline structure of these films was investigated by WAX. Figure 1 shows WAX scans for solution-cast films of PNA–PMMA containing various concentration of PNA. Curves (A) to (E) correspond to PNA concentrations of 10, 18, 30, 40, and 45%, respectively. Figure 2 shows X-ray diffraction (XRD) of pure PNA without any polymer crystallized from acetone. The comparison of these curves clearly brings out the effect of polymer on the structure of these crystals. It is seen that with the increase of polymer content, the major reflections occurring in the 2θ region of 10 to 25 degrees decrease considerably; and, interestingly, there are few new diffraction peaks appearing, even at low concentration, which become more prominent at or above a certain concentration of PNA (30%). At low concentration ($<$18%), the size of the crystals are too small to be detected by X-ray. Although there are major changes in the intensities of the various diffraction peaks, many of them can be assigned to various reflections from PNA itself, with PMMA being amorphous. The comparison of relative intensities of these various peaks has been made in Table I, which also indicates the d-values estimated from these scans. The detailed analysis of the results show that most of the reflections correspond to monoclinic crystalline phase of free PNA with (a) equal to 12.33 Å; (b) 6.07 Å; (c) 8.59 Å; and (β) 91.45°. The new diffraction peaks that become prominent at a certain composition above 30 wt % of PNA, especially, the peak at 2θ = 24.1, could not be assigned to any of the reflection from the monoclinic structure of PNA. Hence, these peaks must correspond new crystalline structure formed, possibly due to a complex between PNA and PMMA. The detailed analysis indicated that these correspond to an orthorhombic crystalline phase with (a) equal to 14.7 Å, (b) equal to 11.0 Å, and (c) equal to 9.0 Å. It is interesting to note that at a low concentration of PNA, a strong reflection occurs, which corresponds to the 020 reflection of monoclinic structure of PNA. It may be noted that this reflection is normally much weaker than the

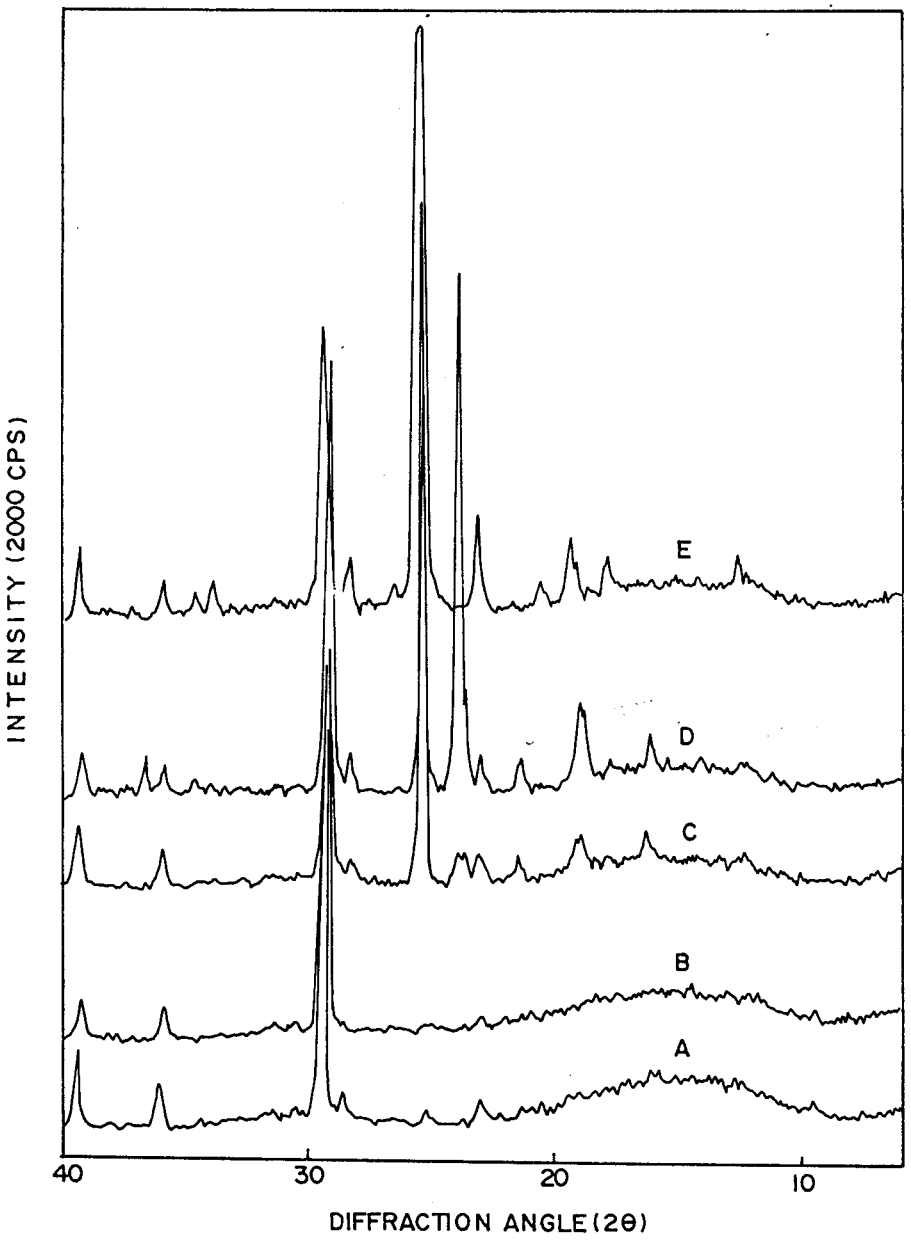

Figure 1 WAX scans for solution-cast films of PNA–PMMA with various concentrations of PNA. Curves (A) to (E) correspond to PNA concentrations of 10, 18, 30, 40, and 45% by weight, respectively.

012 reflection in the case of pure PNA. Such variation in the intensity for diffraction peak could be due to either preferential growth of crystallite along a certain face or to orientation of crystallites with respect to the film surface.

The melt-crystallized samples also show major changes in the intensities of various diffraction peaks, as depicted in the WAX (Fig. 3). In this case also, the presence of polymer matrix during the melt crystallization process has a profound effect on the intensities of 020 and 012 reflections from the monoclinic crystalline phase of PNA. Even in this case, new peaks are observed for PNA concentrations greater than 40%, which do not correspond to any of the possible reflections from the monoclinic type of crystalline structure, as depicted for pure PNA. The new reflections can be assigned according to a new crystal structure, that is, the orthohombic phase of PNA. The comparison of relative intensities of various peaks

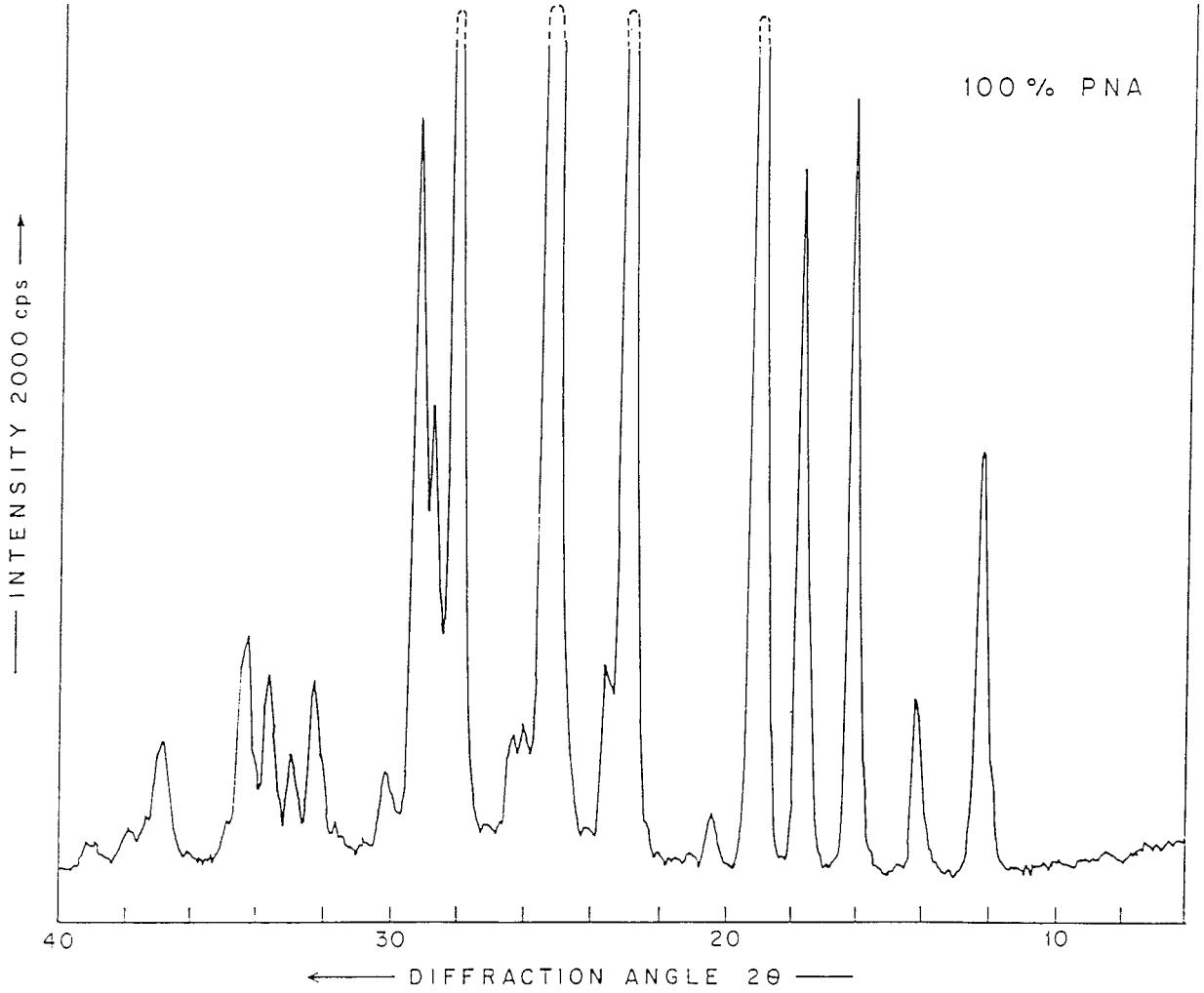

Figure 2 WAX scan for pure para nitroaniline.

and the *d*-values estimated have been assigned in Table II.

The strong influence of the growth condition on the structure development of these crystals is seen from Figure 4, which shows XRD scans for PNA–PMMA composite films having the same concentration (30%) of the additive but grown under melt (curve M), solution (curve S), and with applied field (curve E). The drastic reduction of the reflection from 012 and tremendous increase of the intensity from the 020 plane is noticed when the growth takes place in the presence of an electric field. The detailed analysis of these patterns is given in Table III.

The most interesting part of the present experiments was seen in the effect of crystallization process on the transparency of the films. The photograph in Figure 5 compares the transparency of the films having same composition (40% PNA) but grown from solution (S), that from melt (M), and in the presence of electric field (E). The dark line is clearly revealed through the E films, while the S films are totally opaque. Thus, the effect of oriented growth of the crystals drastically changes the optical qualities of these materials, which are important for their applications in optoelectronics.

In order to investigate the type of interaction between the PNA and PMMA molecules, the infrared (IR) spectra were recorded for these films. Table IV gives the comparison of the different IR bands observed for pure PMMA, pure PNA, and PNA–PMMA, respectively. The additional bands occurring in the region of 3374 to 2362 cm^{-1}, together with significant shift in the carbonyl band (1720–1740 cm^{-1}) for the latter case strongly suggest hydrogen bonding between the two molecules, which would be expected to take

Table I X-ray Diffraction in PNA–PMMA Film Grown by the Solution-Cast Technique

PNA 100%			10%		18%		30%		40%		45%			
d (obs)	I/Io	hkl[a]	*d* (obs)	I/Io	*d* (obs)	I/Io	*d* (obs)	I/Io	*d* (obs)	I/Io	*d* (obs)	I/Io	*d* cal[b]	hkl
7.19	15	101	7.08	7	7.08	11	7.08	8	7.19	8				
											6.97	3	6.97	011
6.23	7	200			6.11	16	6.23	8					6.29	111
									5.71	8			5.69	201
		110					5.41	12	5.47	12			5.50	020
4.983	25	011					4.95	7	4.98	8	4.92	3	4.95	300
							4.67	11	4.69	15			4.69	021
4.64	54	111					4.62	10	6.64	16				
											4.55	4	4.50	002
4.33	3	210	4.33	6										
		300					4.15	5						
							4.11	8	4.13	8			4.16	012
3.85	54	211	3.85	7	3.86	12	3.85	7	3.85	8	3.82	5	3.84	202
3.77	8	301					3.75	7	3.75	18				
							3.69	7	3.70	82			3.65	400/320
3.59	<u>100</u>	012	3.52	5			3.49	<u>100</u>	3.50	<u>100</u>	3.48	<u>100</u>	3.48	022
3.42	6	310												
3.37	6	112									3.33	2	3.38	122
3.16	52	311					3.14	6	3.15	8	3.14	3	3.15	222
3.08		212	3.12	9					3.06	67			3.08	231
3.04	29	020	3.03	<u>100</u>	3.04	<u>100</u>	3.04	55			3.03	15	3.05	420
		021	2.84	5	2.85	10								
2.77	8	121												
2.71	6	220												
2.65	9	411							2.64	3	2.63	2	2.63	023/041
2.60	10	013/203							2.59	4	2.58	1	2.58	141
			2.49	10	2.50	14	2.50	7	2.51	6	2.50	2	2.49	313

[a] Assigned as per monoclinic structure (see the literature[23,24]): (a) 12.33 Å; (b) 6.07 Å; (c) 8.59 Å; (β) 91.45°.
[b] As per new structure (orthorhombic): (a) 14.7 Å; (b) 11.0 Å; (c) 9.0 Å; (β) 90°.
Underlined peaks correspond to reflection of maximum intensity.

place at the amino group of PNA and the C═O group of PMMA. It is also interesting to note from the table that the presence of three C═O frequencies occurring at around 1710, 1726, and 1740 cm^{-1} and a shift in the nitro group of PNA from 1490 cm^{-1} in PNA to 1498 cm^{-1} in PNA–PMMA film clearly suggests the formation of complex between PNA and PMMA and crystallization in new structure (orthorhombic), together with the original monoclinic crystalline phase of PNA. Thus, the complex formation between PNA and PMMA, and its crystallization appears to be a very strong possibility.

The DSC analysis also indicated a few new features, which suggested the presence of a new phase of the material in PNA–PMMA films. Figure 6 depicts the DSC graph of pure PNA and PNA–PMMA composite with 45 wt % additive. Pure PNA shows a sharp melting point at 150.1°C. On the other hand, the composite film exhibits two melting points at 78.6 and 138.2°C, respectively, which could be due to the formation of two types of crystalline phases. It may be mentioned that the higher melting point of 138.2°C corresponds to that of free PNA in the films. The lowering of melting point as compared to pure PNA can be attributed to dilution effect, which, of course, presumes large interaction and good miscibility of components. The presence of another new melting peak (78.6°C) clearly indicates the formation of new crystalline phase, which has already been mentioned in the WAX analysis and corresponds to the orthorhombic phase of the complex. These observations essentially confirm the above hypotheses.

The morphology of these composite films was observed by optical polarizing microscopy and various morphological features are revealed in the photomicrographs in Fig. 7(a)–(d). The pure PMMA films were totally isotropic, showing no

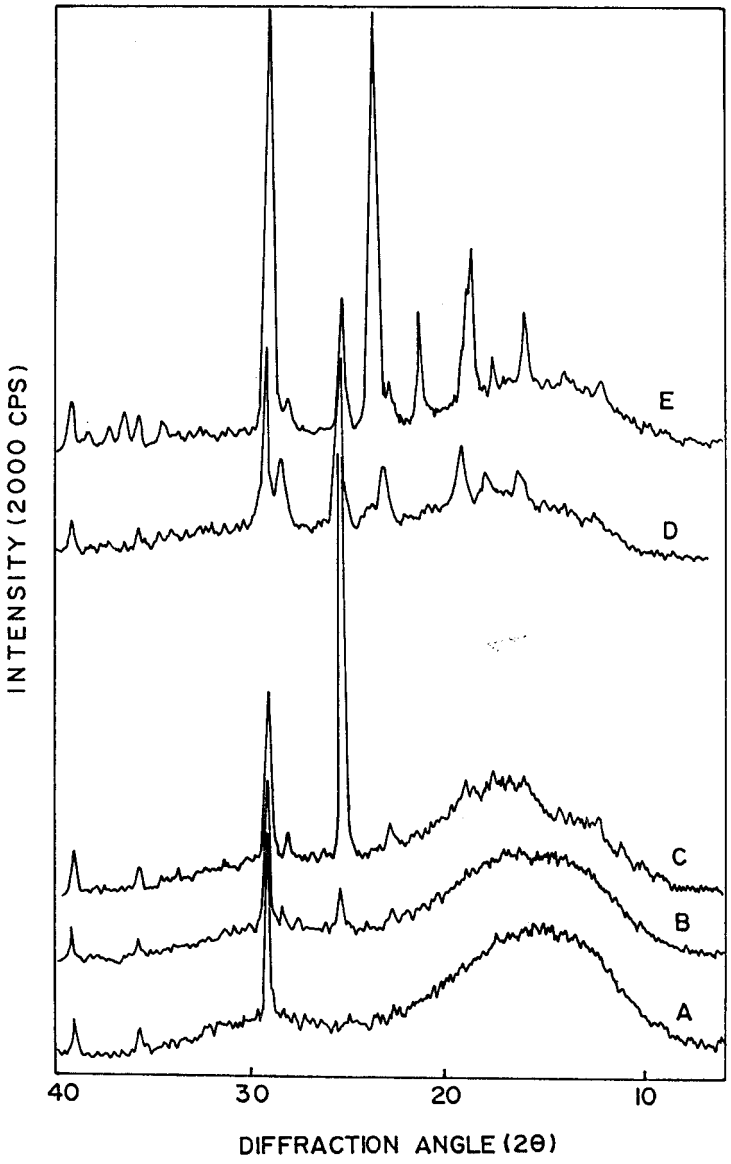

Figure 3 WAXD scans for melt-crystallized films of PNA–PMMA with various concentrations of PNA. Curves (A) to (E) correspond to PNA concentration of 10, 18, 30, 40, and 45% by weight, respectively.

crystallinity or orientation. On the other hand, with the incorporation of PNA, these films showed increasing degree of transmittance under crossed polar condition, suggesting the presence of birefringence and anisotropy. At a low concentration of PNA, the sample predominantly consisted of very small crystals, that is, $\leq 1\ \mu$, appearing as dots [Fig. 7(b)]. The small crystals are due to complex crystallizing in orthorhombic phase of PNA. It is also interesting to note that at a certain critical concentration (30%), both small and large spherulites are observed [Fig. 7(c)]. The small spherulites are seen with intense colors corresponding to new crystalline complex (orthorhombic), while the large spherulites are due to original PNA structure (monoclinic). For very high concentrations of PNA (45%), both spherulitic as well as dendritic morphology [Fig. 7(d)] was noted with spherulitic morphology due to new crystalline complex and the dendritic due to original monoclinic structure of PNA. It may be mentioned here that pure PNA crystals (grown

Table II X-ray Diffraction in PNA–PMMA Film Grown by the Melt-Crystallized Technique

PNA 100%			10%		18%		30%		40%		45%			
d (obs)	I/Io	hkl[a]	*d* (obs)	I/Io	*d* (obs)	I/Io	*d* (obs)	I/Io	*d* (obs)	I/Io	*d* (obs)	I/Io	*d* cal[b]	hkl
7.19	15	101					7.19	7	7.08	11	7.19	6		
6.23	7	200					6.15	7			6.23	6	6.29	111
5.47	28	110					5.47	10	5.37	25	5.47	16	5.50	020
4.98	25	011	5.03	18			4.98	11	4.90	22	4.98	10	4.95	300
											4.69	27	4.69	021
4.64	54	111	4.57	14			4.64	10	4.59	38	4.64	20		
4.33	3	210												
											4.13	18	4.16	012
3.85	54	211					3.85	7	3.81	38	3.85	11	3.84	202
3.77	8	301									3.75	44		
											3.69	100	3.68	400
		202	3.55	13										
3.49	100	012			3.48	38	3.48	100	3.48	93	3.49	23	3.48	022
3.42	6	310												
3.37	6	112												
		312			3.22	24							3.25	411
3.16	52	311					3.15	12			3.15	8	3.15	222
3.08	21	212			3.12	30	3.07	38	3.12	49	3.07	86	3.08	231
3.05	29	020	3.05	100	3.04	100			3.05	100			3.05	420
2.95	4	120												
2.77	8	121												
		410									2.73	4	2.75	412
2.71	6	220												
2.65	9	411					2.65	6	2.63	11			2.63	023/232
2.60	10	013/203							2.57	11	2.59	4	2.59	141
			2.50	14	2.50	14	2.50	6	2.50	12	2.50	5	2.49	313
											2.46	5	2.46	502
2.43	6	122												

[a] As per monoclinic structure: (a) 12.33 Å; (b) 6.07 Å; (c) 8.59 Å; (β) 91.45°.
[b] As per new structure (orthorhombic): (a) 14.7 Å; (b) 11.0 Å; (c) 9.0 Å; (β) 90°.
Underlined peaks correspond to reflection of maximum intensity.

from acetone) have a needle-shaped growth habit [Fig. 7(a)]. These various results clearly indicate that the presence of PMMA as the surrounding matrix affects the crystalline morphology of PNA.

Modifications of crystalline structure and morphology due to different techniques of crystallization have been known in the past.[25] In particular, the presence of impurities during the process of crystallization from solution affects the crystal growth habits, which has been well documented in the literature.[26,27] However, the influence of the surrounding matrix or polymer-induced crystallization is a new observation reported only recently.[17–19] For example, various inorganic salts, such as copper chloride, calcium chloride, potassium carbonate, and cadmium sulphide, have been grown in polymer matrix *in situ* of polyethylene oxide (PEO). The influence of the polymer on the crystallization was found in either new morphological features or change of crystalline phase. This has been attributed to the strong tendency of PEO for complexation with a number of inorganic salts or ions. In a noninteractive system, in which the polymer and the additive are inert, little influence would be expected on crystallization behavior of either component. In the present case, it may be noted that PNA has a very strong dipole moment (13.4 D) due to positively charged amino group placed at the para position of the negatively charged nitro group in the PNA molecule. PMMA has comparatively weak dipole moment associated with its acetate group (6.0 D), and, also, it is wholly amorphous. Thus, one expects the interaction between these two moieties only through the amino group of PNA and carbonyl group of PMMA. Such an interaction is

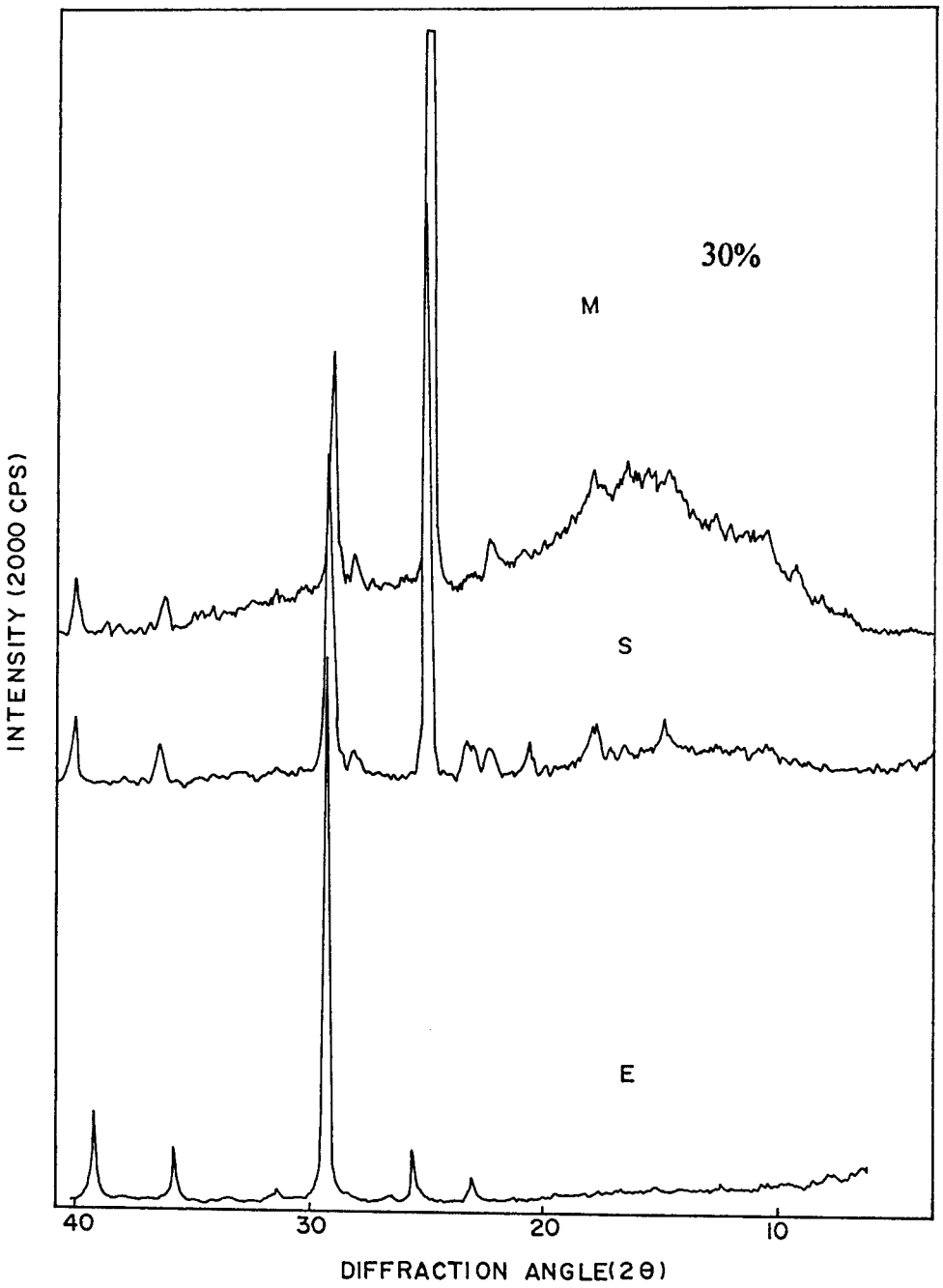

Figure 4 WAXD scans for PNA–PMMA composite film containing 30 wt % PNA and grown by different techniques: melt (curve M), solution (curve S), and crystallized under applied field (curve E).

sufficient to cause the displacement of the PNA molecules during their crystallization. In pure PNA, having a monoclinic crystal structure, all the benzene rings are placed in a planar configuration along the plane parallel to *b*-axis, and any change in these can cause preferential growth, occurrence of new reflections, and modification of growth habit and orientation. This has been indeed observed by us, as indicated above. Interestingly, the application of electric field during crystallization can also cause orientation of these molecules because of their strong dipole moment. Such an orientation induced by electric field will subsequently lead to oriented growth of crystal-

Table III X-ray Diffraction in PNA–PMMA Film (30%) Grown by Various Techniques

Solution-Cast			Melt-Crystallized			Electric Field		
d (obs)	I/Io	hkl	*d* (obs)	I/Io	hkl	*d* (obs)	I/Io	hkl
7.08	8	101	7.19	7	101			
			6.15	7	200			
5.40	11	020[b]	5.47	10	110/020[b]			
4.95	7	011/300[b]	4.98	11	011/300[b]			
4.67	11	021[b]						
4.62	10	111	4.64	10	111			
4.15	5	300						
4.11	8	012[b]						
3.85	7	211/202[b]	3.85	7	211/202[b]	3.86	5	211/202[b]
3.69	7	400[b]/320[b]						
3.49	<u>100</u>	012/022[b]	3.48	<u>100</u>	012/022[b]	3.49	11	012/022[b]
						3.35	2	112
3.14	6	311/222[b]	3.15	12	311/222[b]			
			3.07	38	212/231[b]			
3.04	55	020/420[b]				3.03	<u>100</u>	020/420[b]
						2.84	3	003
2.50	7	313[b]	2.50	6	313[b]	2.50	10	313[b]
						2.29	17	510

[b] As per new structure given in Table I.
Underlined peaks correspond to reflection of maximum intensity.

lites. The presence of one strong reflection (020 plane) for the films crystallized under electric field clearly shows the orientation of the *b*-axis. It is interesting to note that at certain compositions, spherulitic morphology was observed, which would be normally expected for semicrystalline polymers, as, for example, polyethylene oxide dispersed with PNA.[27,28] In such polymers, the polymer molecules passes through the crystalline and amorphous domains and form spherulites; and PNA resides in the intercrystalline zones, while, in the present case, the PNA forms the crystallizing component with PMMA inclusions in the amorphous regions. The PNA–PMMA complex could also crystallize in spherulitic morphology. Such a crystallization behavior has been reported for a number of PEO complexes with inorganic salts as well as urea.[29] These also exhibit spherulitic morphology, different melting points, and new crystalline structures in a similar manner as observed in the present case.

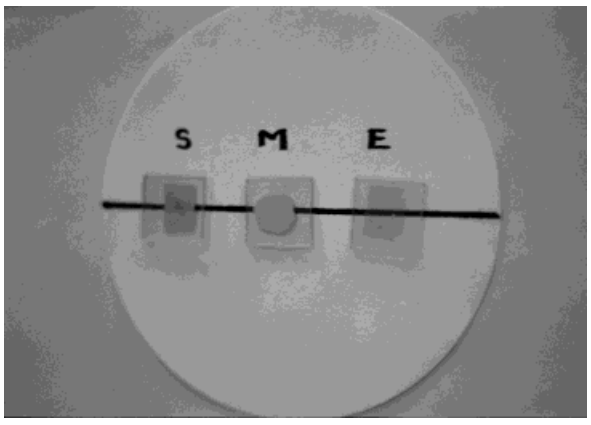

Figure 5 Photograph of samples made by different techniques showing the transparency of the films having same composition (40% PNA): grown from solution (S), melt (M), and electric field (E). The dark line is easily seen through (E).

SUMMARY AND CONCLUSION

The structure and morphology of PNA dispersed in PMMA were studied in order to bring out polymer-induced crystallization and its effects on the growth of the optically active crystals. It was noted from optical microscopy that pure PMMA is isotropic, showing no crystallinity. However, with the incorporation of PNA the films showed a pro-

Table IV IR Absorption of PNA–PMMA 30% Film as Compared with Pure Components

PMMA	PNA	PNA–PMMA	Remarks
	3500 (ms)	3468 (ms)	
	3360 (s)	3374 (vs)	N—H stretch and hydrogen bonding
	3200 (vvw)	3354 (w)	
3050 (w)	2900 (s)		
2995 (ms)	2800 (sh)	2996 (ms)	
		2952 (vs)	CH_2—O deformation
		2842 (vvw)	
2362 (ms)			
1723 (vvs)		1742 (vvs)	
		1720 (vvs)	C═O
		1710 (vvs)	
	1625 (s)	1636 (ms)	Phenyl deformation
	1590 (s)	1598 (vvs)	
	1490 (sh)	1498 (ms)	NO_2 assymetric stretch
		1490 (ms)	
	1475 (s)		
1450 (ms)			CH_2 deformation
	1440 (sh)		Aromatic 1,4-disubstituted
1380 (w)	1390 (sh)	1388 (w)	
	1360 (sh)	1352 (sh)	CH_2 wagging
	1320 (sh)	1326 (vvs)	NO_2 assymetric stretch
1260 (sh)	1280 (vvs)	1274 (vs)	C—N stretch in aromatic
1238 (ms)		1246 (vvs)	O ‖
		1200 (vvs)	C—OR stretch
1180 (ms)		1184 (vvs)	
		1174 (vvs)	C—O—C deformation
1140 (s)	1136 (sh)	1144 (s)	CH_2 wagging, in plane phenyl deformation
	1110 (s)	1110 (vvs)	
1065 (sh)		1064 (sh)	
			δ CH out of plane deformation of aromatic
985 (w)	995 (vvw)	990 (ms)	ring
965 (w)	965 (vvw)	966 (ms)	
	955 (vvw)		
			δ CH out of plane deformation of aromatic
840 (w)	840 (ms)	860 (sh)	ring
		844 (ms)	
823 (w)	820 (sh)		
810 (w)		816 (w)	CH_2 rock

nounced degree of crystallinity, thus showing the presence of anisotropy and birefriengence. The PNA–PMMA films grown by the solution technique showed absence of many reflections in the 2θ range of 10 to 25°, which were dominant in pure PNA. Also, it was observed that only one strong single reflection occurred for 10% concentration of PNA and which corresponds to 020 plane. In addition, it also showed the presence of new reflections, which crystallized in the new crystalline phase of PNA. The melt-crystallized samples, on the other hand, showed profound effects of PMMA on the intensities of 020 and 012 reflections. Further, the occurrence of new diffraction peaks at high concentrations of PNA correspond to complex formation between PNA and PMMA, which crystallized in new orthorhombic crystalline structure. The electric field applied for

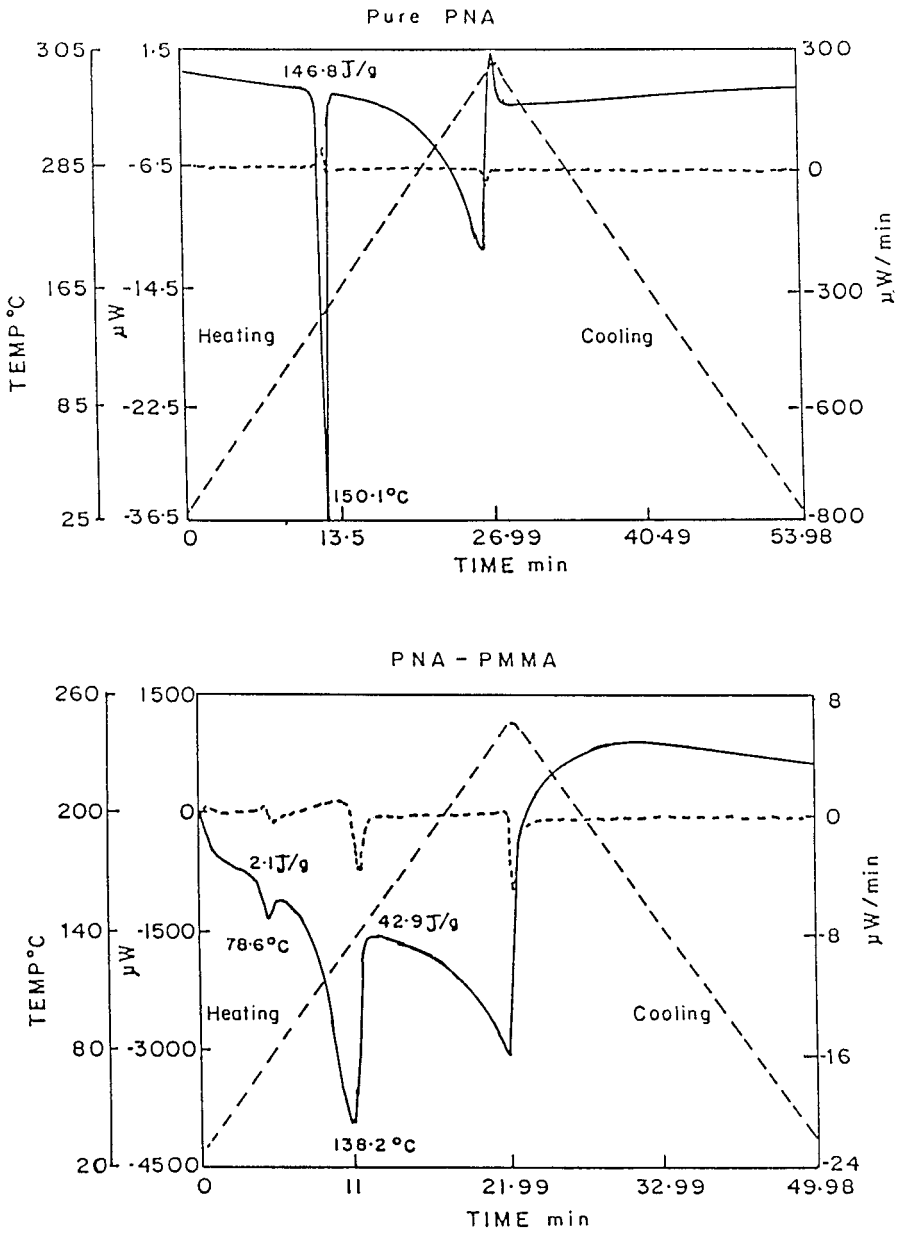

Figure 6 DSC thermograms of pure PNA and PNA–PMMA films containing 45 wt % PNA.

30% PNA–PMMA film showed a dramatic increase of intensity of 020 plane. The spherulitic growth morphology was observed for a certain critical concentration (30% and 40% PNA–PMMA film), as compared to needle-shaped crystals for pure PNA. This spherulitic growth was due to the incorporation of PMMA in the intercrystallite domains.

These studies clearly demonstrate that it is possible to control the orientation, growth, and crystalline phase of an optically active material (PNA) dispersed in a polymer by using molecular interaction between the matrix host and the dopant guest molecules. By application of electric field during crystallization, it is possible to induce orientation of not only the molecules, but also the subsequently grown crystals. Further, these films showed transparency with the application of electric field. Hence, it may be possible to obtain high transparency, even at a

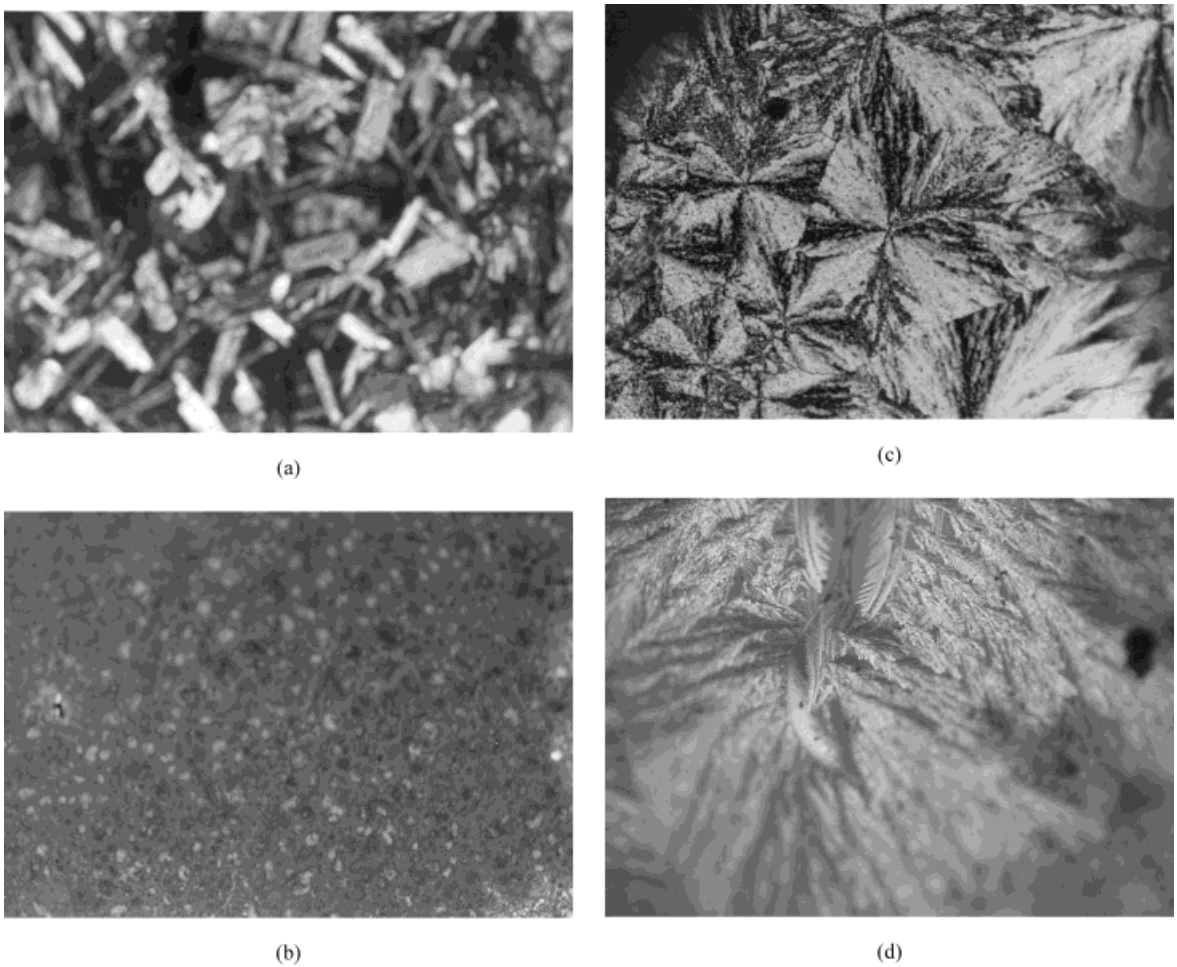

Figure 7 Optical micrograph for (a) pure PNA, (b) solution-grown PNA–PMMA (30%), (c) PNA–PMMA (40%), and (d) PNA–PMMA (45%).

high concentration of PNA if proper orientation of the crystallites is induced in the same. This can lead to improvements in their optical properties as well.

REFERENCES

1. Jones, A.; Hills, J. R.; Pantelius, P. in High Value Polymers; Fawcett, A. H., Ed.; RSC: London UK, 1991; p. 241.
2. Yashino, K. Synth Metals 1989, 28, C669.
3. Colvin, V. L.; Schlaup, M. C.; Alivisatos, A. P. Nature 1994, 370, 354.
4. Munn, R. W.; Ironside, C. N. Principles and Applications of Non-Linear Optical Materials; Blackie: London, UK, 1993.
5. Chilton, J. A.; Goosey, M. T. Special Polymers for Electronics and Optoelectronics; Chapman & Hall: London, UK, 1995.
6. Bowden, M. J.; Turner, S. R. Electronic and Photonic Applications of Polymers; ACS: Washington, DC, 1988.
7. Williams, D. J. Non-Linear, Optical Properties of Organic and Polymeric Materials; ACS: Washington, 1983.
8. Izawa, K.; Okamoto, N. Mol Cryst Liq Cryst 1992, B3, 247.
9. Matsushima, R.; Takeshita, H.; Okamoto, N. J Mater Chem 1991, 4, 591.
10. Cheng, G.; Xu, Y.; Wang, W.; Feng, Z.; Wang, X.; Wen, J. Polym Int 1994, 35, 273.
11. Pauley, M. A.; Guan, H. W.; Wang, H. J Chem Phys 1996, 104, 6834.
12. Silence, S. M.; Hache, F.; Doncker, M.; Walsh, C. A.; Bjorklund, G. C.; Tweig, R. J.; Moerner, W. E. Proc SPIE–Int Soc Opt Eng 1993, 1852, 253.
13. Mann, S.; Archibald, D. D.; Didymus, J. M.; Douglas, T.; Heywood, B.R.; Meldrum F.-C.; Reeves H. J. Science 1993, 261, 1286.

14. Wittmann, J. C.; Smith, P. Nature 1991, 352, 414.
15. Radhakrishnan, S.; Schultz, J. M. J Cryst Growth 1992, 116, 378.
16. Radhakrishnan, S.; Saini, D. R. J Cryst Growth 1993, 129, 191.
17. Radhakrishnan, S. J Cryst Growth 1994, 141, 437.
18. Radhakrishnan, S.; Nadkarni, V. M. Int J Polym Mater 1986, 11, 79.
19. Radhakrishnan, S.; Joshi, S. G. Eur Polym J 1987, 23, 819.
20. Radhakrishnan, S.; Joseph, Roy Ferroelectrics 1993, 142, 189.
21. Pamplin, B. R. Crystalline Growth; Pergaman Press, Elmsford, NY, 1975.
22. Gilman, J. J. Art and Science of Growing Crystals; J. Wiley: New York, 1963.
23. ASTM Diffraction Files 1-0585, ASTM, Washington, DC, 1962.
24. Wyckoff, W. G. Crystal Structures, Vol. 6; John Wiley: New York, 1969; p. 122.
25. Ueda, R.; Mullins, J. B. Crystal Growth and Characterization; North Holland Publishing Co.: Amsterdam, The Netherlands, 1974.
26. Jackson, K. A.; Mullin, J. B. Crystal Growth; North Holland Publishing Co.: Amsterdam, The Netherlands, 1974.
27. Saujanya, C.; Radhakrishnan, S. J Appl Polym Sci 1997, 65, 1127.
28. Watanbe, T.; Yoshigara, K.; Fichou, D.; Miyata, T. J Chem Soc, Chem Comm 1988, 250.
29. Tadokoro, H.; Yoshihara, T.; Chatani, Y.; Murahashi, S. J Polym Sci, Part B: Polym Phys 1964, 2, 263.